






Simultaneous construction of axial and planar chirality by gold/TY-Phos-catalyzed asymmetric hydroarylation

Pei-Chao Zhang ¹, Yin-Lin Li ¹, Jiafeng He ¹, Hai-Hong Wu ¹✉, Zhiming Li²✉ & Junliang Zhang ^{2,3}✉

The simultaneous construction of two different chiralities via a simple operation poses considerable challenge. Herein a cationic gold-catalyzed asymmetric hydroarylation of ortho-alkynylaryl ferrocenes derivatives is developed, which enable the simultaneous construction of axial and planar chirality. The here identified TY-Phos derived gold complex is responsible for the high yield, good diastereoselectivity (>20:1 dr), high enantioselectivities (up to 99% ee) and mild conditions. The catalyst system also shows potential application in the synthesis of chiral biaryl compounds. The cause of high enantioselectivity of this hydroarylation is investigated with density functional theory calculation.

¹Shanghai Key Laboratory of Green Chemistry and Chemical Processes, School of Chemistry and Molecular Engineering, East China Normal University, Shanghai, China. ²Department of Chemistry, Fudan University, Shanghai, China. ³State Key Laboratory of Organometallic Chemistry, Shanghai Institute of Organic Chemistry, CAS, Shanghai, China. ✉email: hhuw@chem.ecnu.edu.cn; lizm@fudan.edu.cn; junliangzhang@fudan.edu.cn

As an effective and exceptionally versatile strategy, the development of catalytic asymmetric intramolecular hydroarylation for the construction of axial^{1–10} and planar^{11–13} chirality or helicenes^{14–20} has received much attention^{21–32}. Various transition metal catalysis involving Au, Pt, Rh, and Pd, have been reported in this regard. For instance, the groups of Alcarazo^{1,14,16,18} and Tanaka^{6,15,17} extensively studied the Au-catalyzed and Rh-catalyzed intramolecular alkyne hydroarylation to achieve enantioselective synthesis of axially chiral biaryls and helicenes, respectively (Fig. 1a). In 2013, Uemura et al.¹⁰ developed a Pd-catalyzed asymmetric cycloisomerization of enynes for the construction of axially chiral biaryl. The group of Urbano and Carreño¹¹ developed an Au-catalyzed cyclization to construct the planar naphthalene-fused ferrocenes in 2016 (Fig. 1a). Later, Shibata et al.¹² reported the similar reaction enabled by a Pt-catalysis. Meanwhile, the capacity of intramolecular hydroarylation is impressively complemented by various other versatile stereocontrolled methodologies. For example, Shibata² and co-workers reported a Rh-catalysed enantioselective synthesis of axially chiral PAHs via regioselective cleavage of biphenylenes. Stará and Starý^{19,20} developed a Ni-catalysed enantioselective [2 + 2 + 2] cycloisomerisation of aromatic triynes to obtain the helicene derivatives. Toullec³, Yan⁴, Irie⁵, and Sparr^{7–9} independently demonstrated efficient organocatalytic enantioselective cyclization of aryl-alkynes to construct valuable molecules containing axial or axial and helical stereogenic elements.

In this work, the simultaneous construction of axial and planar chiralities is realized via the gold-catalyzed^{33–42} asymmetric intramolecular hydroarylation of readily available o-alkynylferrocene derivatives **1**⁴³ (Fig. 1c). And the simultaneous construction of two different types of chiralities is now flourishing development (Fig. 1b)^{44–51}.

Results

Optimization of the reaction conditions. However, to the best of our knowledge, simultaneous construction of multiple chiralities by asymmetric gold catalysis has not been reported so far, this hypothesis faced considerable challenges: (1) the universal and efficient asymmetric intramolecular desymmetric cyclization for the construction of planar ferrocene derivatives was not well developed (In the work of refs. ^{11,12}, 10–20 mol% catalytic loading was used), (2) on the other hand, simultaneous construction of axial and planar chiral molecules via asymmetric catalysis has rarely been reported^{52,53} and innate reluctance to

undergo a related asymmetric desymmetric aromatization, and (3) the inherent difficulties to asymmetric gold catalysis, which stem from its linear coordination geometry and the outer-sphere nature of Au(I)-catalysis^{44–50}. To test our hypothesis, our investigation began with the cyclization of ortho-alkynylaryl ferrocene derivative **1a**. A series of commercially available chiral ligands were investigated (please find more details in the Supplementary Information (SI) Supplementary Fig. S3). Unfortunately, catalysts used by Urbano-Carreño¹¹, Shibata¹², or Uemura¹⁰ all failed to give the desired cyclization product (Fig. 2, entries 1–3). (R)-DTBM-SEGPhos (L1), the commonly used chiral ligand in asymmetric gold catalysis, delivered the enantiomer of **2a** in 15% NMR yield with 80% ee and 3:1 diastereoselectivity. (S,S)-Ph-BPE (L2) could give the product **2a** in quite low enantioselectivity and conversion. (R)-BINAP (L3) furnished **2a** in 62% NMR yield with 51% ee and 5:1 d.r., and the dominant Brønsted acid (R)-CPA (L4) in the field of atroposelective synthesis of axially chiral molecules, cyclohexanediamine-derived (S,S)-DACH-Phenyl Trost Ligand (L5), (R)-BI-DIME (L6), Binol-derived phosphor-amidite (S_a,R,R)-CPPA (L7), chiral oxazoline-phosphine ligand (R)-tBu-PHOX (L8), all have insufficient catalytic activity. We next turned to investigate our developed chiral sulfinamide phosphine (Sadphos), which has shown good performance in asymmetric gold catalysis^{41–43} (Sadphos are commercially available (*Daicel and Strem*), which are also easily prepared in 2–4 steps from chiral *tert*-butane sulfinamide.) (Fig. 2). The gold complexes derived from Ming-Phos^{42,43,54–56}, Xu-Phos^{57–61}, Xiang-Phos^{62–65}, PC-Phos^{41,66–68} and TY-Phos⁶⁹ could deliver (–)-**2a** in up to 83% yield with 85% ee. We found that enantioselectivity roughly correlates to the electrical properties of the Sadphos, with a more σ -donating ligand providing a higher enantioselectivity and catalytic activity. Notably, Au(TY-Phos)Cl could be easily synthesized in a gram scale via a five-steps in “one-pot” synthesis (for more details, see the SI). Inspired by this promising result, we varied the Ar group of TY-Phos (TY2–TY4) and introduced electron-donating groups to the aryl moiety of TY-Phos, structured as TY5–TY6 with alkyl groups. Gratifyingly, the product **2a** could be obtained in 83% yield with 85% ee and 5:1 d.r. with the use of [Au(TY5)]BAR^F as the catalyst. Moreover, N-Me-TY5 delivered much lower enantioselectivity to 46% ee (Fig. 2, entry 10). Then, the effect of the counterion was investigated (Fig. 2, entries 8, 11–13)⁷⁰, among which sodium tetrakis [3,5-bis(trifluoro-methyl) phenyl]borate (BAR^{F-}) delivered the best enantioselectivity and reactivity. Subsequently, either lowering the temperature to –10 °C or using other solvents such as DCE and toluene failed to give better result (Fig. 2, entries 14–16).

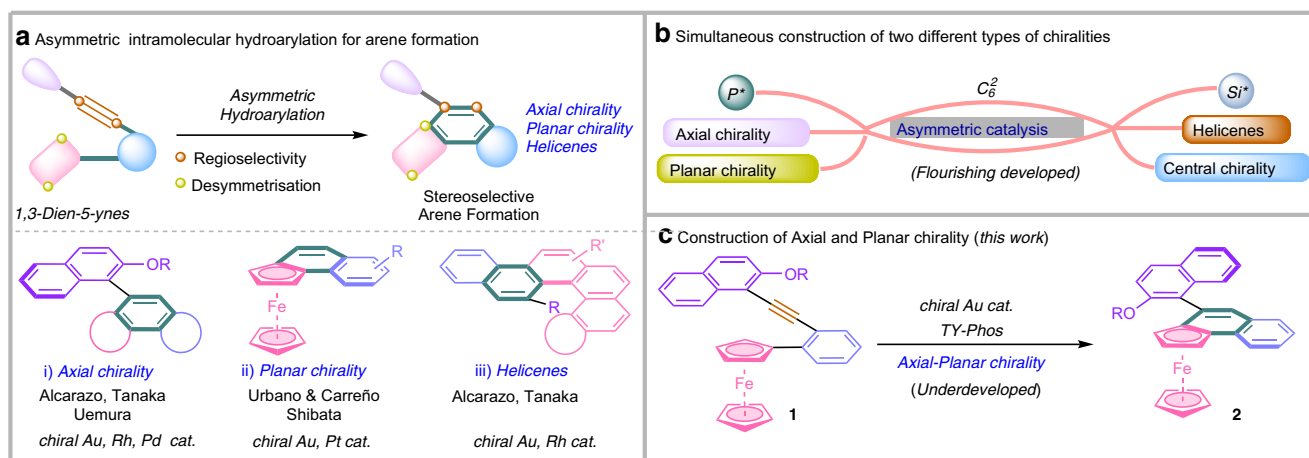


Fig. 1 Background and project synopsis. **a** Asymmetric intramolecular hydroarylation for arene formation. **b** Simultaneous construction of two different types of chiralities. **c** Construction of Axial and Planar chirality (this work).

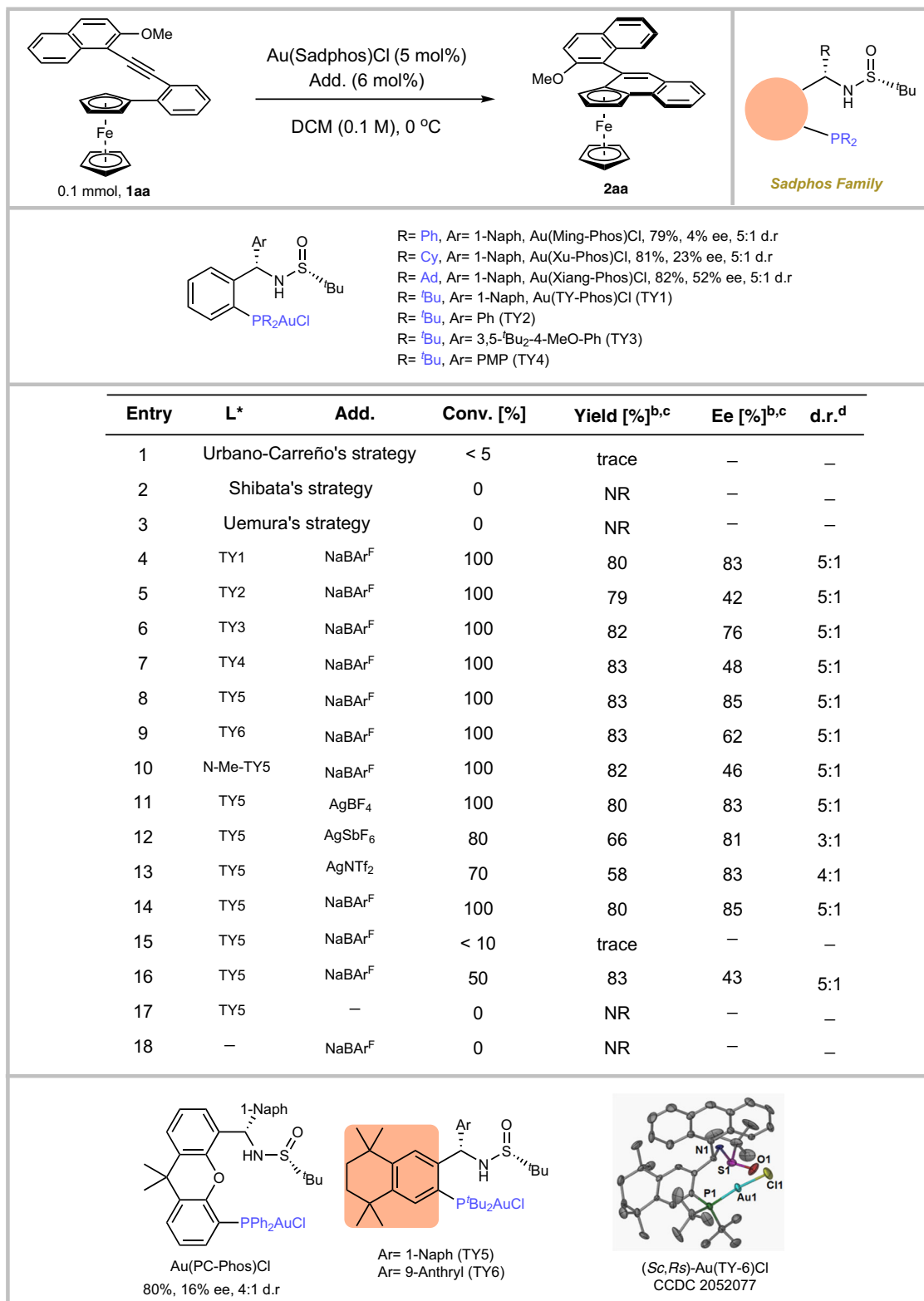


Fig. 2 Optimization of reaction conditions. ^aUnless otherwise noted, all reactions were carried out with 0.1 mmol of **1aa** and 10 mol% of catalyst (Au: P: NaBAR^F (additive) = 1:1:1.2) in 1.0 mL DCM at 0 °C for 24 h; ^bIsolated yield. ^cDetermined by chiral HPLC. ^dDetermined by NMR. ^eAt –10 °C; ^fIn 1.0 mL toluene; ^gIn 1.0 mL DCE. Shibata's strategy: PtCl₂(cod) (10 mol%), (S,S)-Ph-BPE (10 mol%) and AgBF₄ (20 mol%) in DCE at r.t.; Urbano-Carreño's strategy: (R)-DTBM-SEGPhos(AuCl)₂ (10 mol%) and AgSbF₆ (20 mol%) in toluene at 0 °C; Uemura's strategy: [Pd(MeCN)₄](BF₄)₂ (5 mol%) and (R)-Binap (10 mol%) in DCE at 60 °C.

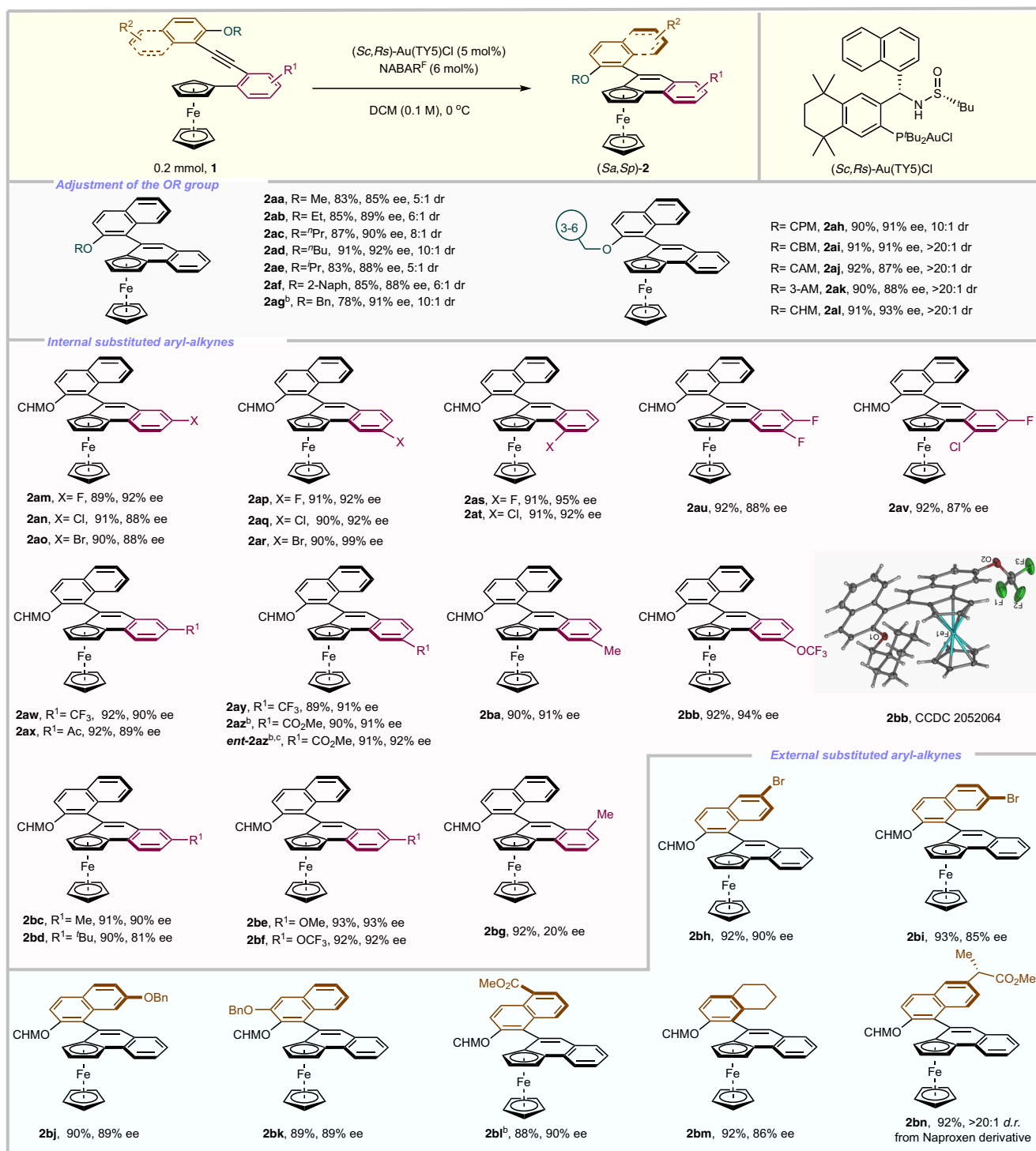


Fig. 3 Exploration of substrate scope. ^aReaction conditions: unless otherwise noted, all reactions were carried out with 0.2 mmol of **1**, Au(TY5)Cl (5 mol %), NaBar^F (6 mol%) in 2.0 mL DCM at 0 °C; isolated yields; the ee values were determined by chiral HPLC, >20:1 dr. ^bAu(TY5)Cl (10 mol%), NaBar^F (12 mol%). ^c(Rc,Ss)-Au(TY5)Cl. CPM Cyclopropylmethyl, CBM Cyclobutylmethyl, CAM Cycloamylmethyl, AM amylmethyl, CHM Cyclohexylmethyl.

Finally, no counterion or only additives which all have not catalytic activity (Fig. 2, entry 18–19).

Reaction scope study. Further optimization focused on adjustment of the OR group. Surprisingly, a meaningful increasing enantioselectivity and reactivity and diastereoselectivity occurred when the R was switched to the longer carbon chains (Fig. 3, **2aa–2ad**). Bulkier groups (OⁱPr, O-2-Naph) could furnish the

corresponding products in 88% ee (**2ae**, **2af**). Better enantioselectivity (92% ee) was achieved with a benzyl (Bn) protecting group (**2ag**), however, the diastereoselectivity and reactivity is still far from ideal. The cyclohexylmethyl (CHM) group seems to be crucial to deliver good result (**2ah–2al**). A series of internal substituted aryl-alkynes were then prepared and tested to this cyclization process. A good tolerance towards halogens (**1am–1av**), electron-withdrawing substituents (**1aw–1az**), electron-withdrawing substituents (**1aw–1az**), electron-donating

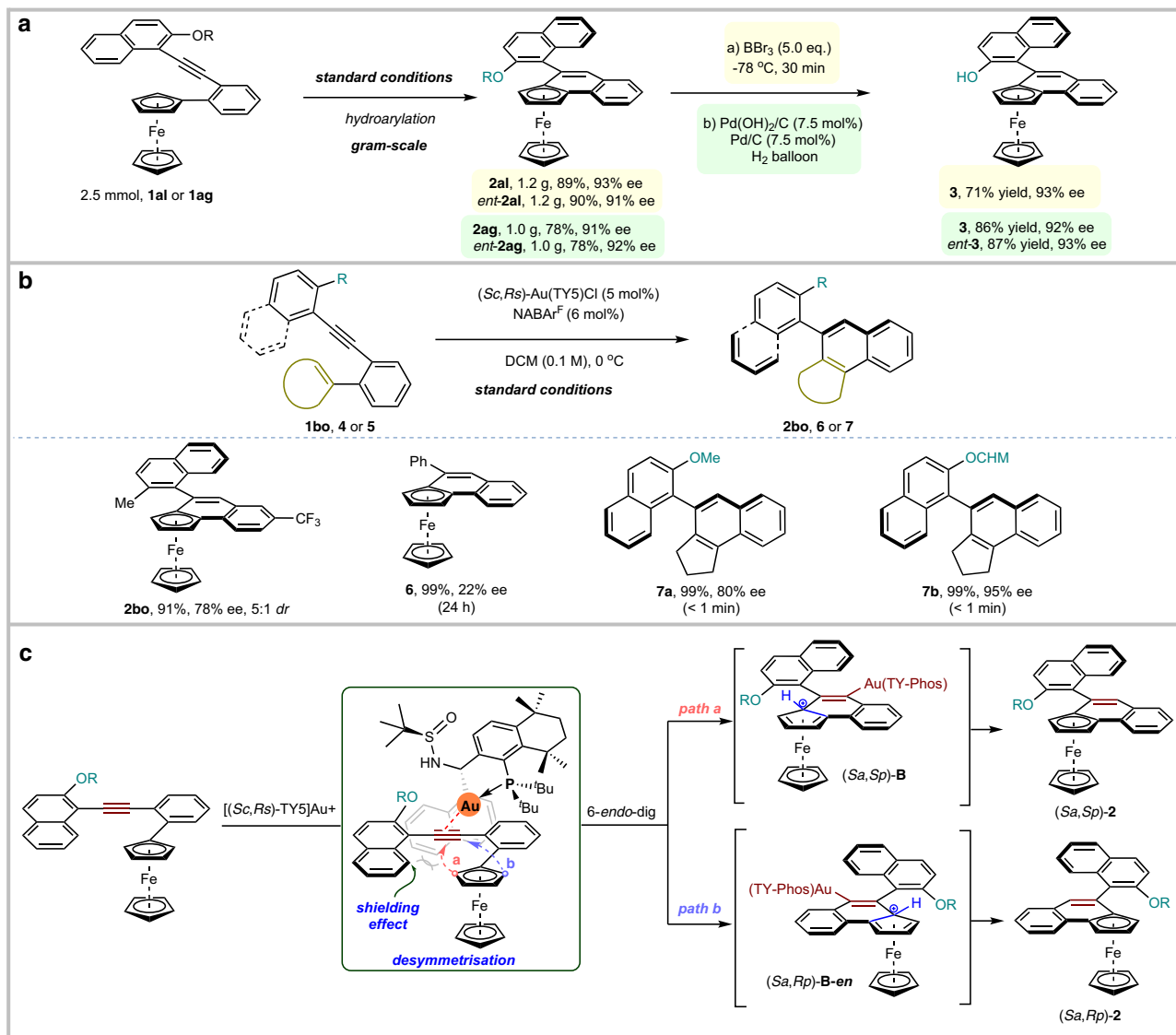


Fig. 4 Proof-of-principle study. **a** The practical utility. **b** mechanism study. **c** proposed asymmetric induction model.

substituents and steric hindrance groups (**1ba–1bf**) on different positions of the phenyl ring (R^1) were observed and the corresponding products (**2am–2bf**) were obtained in 88–92% yields with 81–99% ee. The structure and configuration of (*Sa,Sp*)-**2bb** was unambiguously determined via its X-ray analysis. There is an obvious substituent effect at the *ortho*-position of the aryl alkyne, indicating that the steric hindrance at *ortho*-position is unbeneficial to the enantioselectivity (**2bg**). Gratifyingly, the naphthyl and phenyl ring bearing electron-donating and electron-withdrawing groups at different positions (R^2), could deliver the desired products (**2bh–2bm**) in excellent yields with moderate to high ee. Then, employing the derivative of pharmaceutical naproxen as the substrate **1bn**, the corresponding product **2bn** could be obtained in high yield with excellent diastereoselectivity.

To demonstrate the practical utility of this protocol for synthesis of ferrocene derivatives bearing axial and planar chirality (Fig. 4a), four reactions were carried out in gram scale under standard conditions. With the use of Au[TY5]⁺ and its enantiomer, 1.2 g of **2a** and **ent-2a** were produced in 89% yield with 93% ee and in 90% yield with 91% ee, respectively. 1.0 g of **2ag** and **ent-2ag** were produced in 78% yield, 91% ee and 78% yield, 92% ee, respectively using the same procedure. Dealkylation

of the aryl alkyl ethers **2a** with concentrated boron tribromide led to chiral naphthol **3**⁷¹ in 71% yield 93% ee. Subsequent hydrogenation of aryl benzyl ethers **2ag** and **ent-2ag** with the combination of Pd(OH)₂ and Pd/C in a 1:1 ratio⁷² afforded axial and planar chiral naphthol **3** in 86% yield 92% ee and **ent-3** in 87% yield 93% ee, respectively.

To unravel the origin of the high enantioselectivity of the reaction (Fig. 4b), the asymmetric hydroarylations of 1-ethynyl-2-methylnaphthalene derivative **1a**, 2-benzyne-1-ferrocenylbenzenes **4**, 2-aryne-1-arylbenzenes **5a** and **5b** were also carried out under standard conditions. The **2bo** could be obtained in 91% yield with 78% ee and 5:1 *d.r.*, **6** with only the planar chirality was delivered in 99% yield but with low ee (22% ee), in contrast, axial chiral **7a** and **7b** were obtained in 99% yield with 80% ee and 95% ee, respectively and the reactions were complete in less than one minute. Moreover, the linear relationship (see Supplementary Information (SI), Supplementary Fig. S2) between the ees of the Au(TY5)Cl and those of product **2a** and the e.e. of the **2a** did not significantly change during the reaction, which reveal that the enantioselectivity-determining step might involve a single chiral sulfinamide phosphine ligand and one gold species. In light of the structures of the chiral gold catalyst Au[(*Sc,Rs*)-TY5]⁺ and the product **2**, a

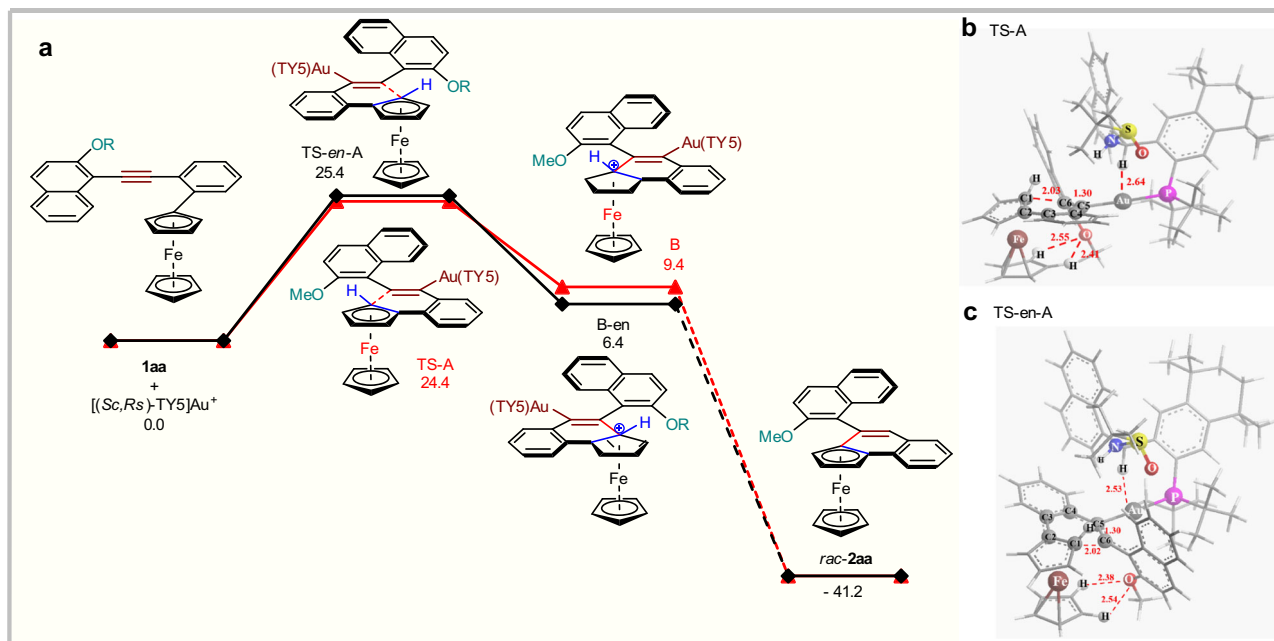


Fig. 5 Density functional theory (DFT) calculations. **a** The Free-energy reaction profiles (kcal mol^{-1}) for the reaction of **1aa**, calculated with SMD Model (dichloromethane) using M062X at 273 K. **b** and **c** The optimized transition states TS-A, TS-en-A for the enantioselectivity-determining step, calculated with SMD Model (Dichloromethane) with M062X method at 273 K.

catalytic chirality-induction model was proposed for the reaction (Fig. 4c). The phosphine of the ligand and the alkyne coordinate to the Au(I) center. The *Re* face of alkyne and the alkoxy group are shielded by the 1-naphthyl group of the ligand and the ferrocene group attack takes place at the *Si* face to define the (*Sp*)-planar chirality (path b), the alkoxy group causes a blockage in the rotation of the naphthalene ring to define the (*Sa*)-axial chiralities. Because of these, it defines to form the product (*Sa,Sp*)-**2** with excellent enantioselectivity and diastereoselectivity.

To shed light on the mechanism of the reaction, especially the planar enantioselectivity determining step catalyzed by Au/(*Sc,Rs*)-TY5, density functional theory (DFT) calculations were carried out with Gaussian 09 software package^{73–75}. The geometry optimization and frequency calculations were carried out with M062X method and combined basis sets. That is, 6–31G (d) for the reactant **1aa** fragment (except the hydrogen atom of the reaction site on the phenyl ring), the heteroatoms P, S, N, O (connected with S atom) on the ligand (*Sc,Rs*)-TY5 and the carbon atoms linked with the above mentioned heteroatoms, SDD for Au and Fe atoms⁷⁶. Considering the existence of hydrogen bonding, 6–31 + G(d,p) basis set was applied for the H atom of the reaction site on the phenyl ring of **1aa** and the H atoms on the chiral carbon and on the N atom of (*Sc,Rs*)-TY5. 3–21 G basis set was used for all the other atoms. Truhlar and co-workers' SMD solvation model was employed to consider the solvent effect of dichloromethane ($\epsilon = 8.93$)⁷⁷. The geometry optimizations were performed without symmetry constraints and the nature of the extrema was checked by analytical frequency calculations. The intrinsic reaction coordinate calculation^{78,79} was also performed to verify the connectivity of the transition state and the energy minima. (see Supplementary Data for details)

The reaction of **1aa** is selected as the model and we focused on the planar enantioselectivity of the reaction (Fig. 5). Enantio-determining step of the reaction is the 6-*endo*-dig cyclization, that is, aromatic ferrocene attacks the alkyne moiety of **1aa**, which is activated by cationic Au/(*Sc,Rs*)-TY5. The following protometalation gives high enantioselective **2aa**. Barriers (TS-A and TS-*en*-A) for the enantioselective step are 24.4 and 25.4 kcal/mol for

the major and minor intermediates B and B-*en*, which means the reaction can proceed smoothly at reaction temperature. In addition, the difference of the two barriers are 1.0 kcal/mol, that is also in good line with the experimental 85% ee value of **1aa** reaction. Both TSs are late transition states, and the structures are closer to those of B and B-*en* (Fig. 5). For example, in both TSs, new 6-membered rings almost formed, C5–C6 distances are 1.30, very similar to that of normal double bonds. Meanwhile, weak interaction can be found between the tertiary hydrogen atom of TY5 and Au atom, the Au–H distances are 2.64 and 2.53 Å, respectively (Fig. 5). The two hydrogen bonds between O atom of the methoxy group and two hydrogen atoms on ferrocene may contribute to the axial enantioselectivity of the reaction. In TS-A, π - π stacking effect was found between two naphthyl groups from TY5 and **1aa** parts respectively, while there is no such effect in TS-*en*-A. This may be the cause of high facial enantioselectivity of the reaction.

In summary, we developed an efficient gold(I)/TY-Phos-catalyzed intramolecular hydroarylation of *ortho*-alkynylaryl ferrocenes derivatives, which represents the highly enantioselective and diastereoselective simultaneous construction of axial and planar chiral (*Sa,Sp*)-naphthalene-fused ferrocene derivatives. The axial biaryl compound could be also delivered efficiently under the same reaction conditions. The here identified cationic Au(TY-Phos)⁺ is responsible for the high yield and diastereoselectivity, good to excellent enantioselectivities. The DFT calculations explained the chirality-induction model and accounts for the high enantioselectivity. We believe that this well-designed, easily available gold catalyst Au(TY-Phos)Cl can be applied in other catalytic asymmetric transformations.

Methods

Typical procedure for simultaneous construction of axial and planar chirality by Gold/TY-Phos-catalyzed asymmetric hydroarylation. In a dried Schlenk tube, after the solution of (*Sc,Rs*)-Au(TY5)Cl (5 mol%, 8.2 mg) and NaBAR^F (6 mol%, 10.6 mg, cas: 79060-88-1, Energy Chemical, white powder) in DCM (0.5 mL) was stirred at room temperature for 15 min. Then the above catalyst solution was added to the solution of **1**, 4–5 (0.2 mmol) in DCM (1.5 mL) at 0 °C. The reaction was determined by TLC analysis, after the **1**, 4–5 was consumed completely. Solvent was removed in a rotary evaporator, purified by flash column chromatography on silica

gel (Hexane/DCM = 10:1 to 5:1) to afford the desired product **2**, **6**, **7**. All new compounds were fully characterized (see the Supplementary Information).

Data availability

The data that support the findings of this study are available within the article, its Supplementary Information files and Supplementary Data files. All data underlying the findings of this work are available from the corresponding author upon reasonable request. The X-ray crystallographic coordinates for structures reported in this study have been deposited at the Cambridge Crystallographic Data Center (CCDC), under deposition numbers 2052064 ((*Sa,Sp*)-**2bb**) and 2052077 ((*Sc,Rs*)-TY6)AuCl. The data can be obtained free of charge from The Cambridge Crystallographic Data Center via http://www.ccdc.cam.ac.uk/data_request/cif.

Received: 26 January 2021; Accepted: 30 June 2021;

Published online: 29 July 2021

References

- Zhang, J., Simon, M., Golz, C. & Alcarazo, M. Gold-catalyzed atroposelective synthesis of 1,1'-binaphthalene-2,3'-diols. *Angew. Chem. Int. Ed.* **59**, 5647–5650 (2020).
- Takano, H., Shiozawa, N., Imai, Y., Kanyiva, K. S. & Shibata, T. Catalytic enantioselective synthesis of axially chiral polycyclic aromatic hydrocarbons (PAHs) via regioselective C–C bond activation of biphenylenes. *J. Am. Chem. Soc.* **142**, 4714–4722 (2020).
- Gicquiaud, J. et al. Brønsted acid-catalyzed enantioselective cycloisomerization of arylalkynes. *Chem. Eur. J.* **26**, 16266–16271 (2020).
- Peng, L. et al. Organocatalytic asymmetric annulation of *ortho*-alkynylanilines: synthesis of axially chiral naphthyl-C2-indoles. *Angew. Chem. Int. Ed.* **58**, 17199–17204 (2019).
- Arae, S. et al. Asymmetric synthesis of axially chiral benzocarbazole derivatives based on catalytic enantioselective hydroarylation of alkynes. *Org. Lett.* **20**, 4796–4800 (2018).
- Satho, M., Shibata, Y., Kimura, Y. & Tanaka, K. Atroposelective synthesis of axially chiral all-benzenoid biaryls by the gold-catalyzed intramolecular hydroarylation of alkynes. *Eur. J. Org. Chem.* **26**, 4465–4469 (2016).
- Lotter, D., Neuburger, M., Rickhaus, M., Häussinger, D. & Sparr, C. Stereoselective arene-forming aldol condensation: synthesis of configurationally stable oligo-1,2-naphthylenes. *Angew. Chem. Int. Ed.* **55**, 2920–2923 (2016).
- Fäseke, V. C. & Sparr, C. Stereoselective arene-forming aldol condensation: synthesis of axially chiral aromatic amides. *C. Angew. Chem. Int. Ed.* **55**, 7261–7264 (2016).
- Link, A. & Sparr, C. Organocatalytic atroposelective aldol condensation: synthesis of axially chiral biaryls by arene formation. *Angew. Chem. Int. Ed.* **53**, 5458–5461 (2014).
- Kadoya, N., Murai, M., Ishiguro, M., Uenishi, J. & Uemura, M. Palladium(II)-catalyzed asymmetric cycloisomerization of enynes for axially chiral biaryl construction. *Tetrahedron Lett.* **54**, 512–514 (2013).
- Urbano, A., Hernández-Torres, G., del Hoyo, A. M., Martínez-Carrióna, A. & Carreño, M. C. Mild access to planar-chiral *ortho*-condensed aromatic ferrocenes via gold(I)-catalyzed cycloisomerization of *ortho*-alkynylaryl ferrocenes. *Chem. Commun.* **52**, 6419–6422 (2016).
- Shibata, T., Uno, N., Sasaki, T. & Kanyiva, K. S. Pt-catalyzed enantioselective cycloisomerization for the synthesis of planar-chiral ferrocene derivatives. *J. Org. Chem.* **81**, 6266–6272 (2016).
- Ito, M., Okamura, M., Kanyiva, K. S. & Shibata, T. Catalytic enantioselective synthesis of azepine-fused planar-chiral ferrocenes by Pt-catalyzed cycloisomerization. *Organometallics* **38**, 4029–4035 (2019).
- Hartung, T., Machleid, R., Simon, M., Golz, C. & Alcarazo, M. Enantioselective Synthesis of 1,12-Disubstituted [4]Helicenes. *Angew. Chem. Int. Ed.* **59**, 5660–5664 (2020). The catalytic asymmetric intramolecular cyclization for the stereoselective helical-arene formation, see.
- Kinoshita, S. et al. Rhodium-catalyzed highly diastereo- and enantioselective synthesis of a configurationally stable s-shaped double helix-like molecule. *Angew. Chem. Int. Ed.* **59**, 11020–11027 (2020).
- Nicholls, L. D. M. et al. TADDOL-derived cationic phosphonites: toward an effective enantioselective synthesis of [6]helicenes via Au-catalyzed alkyne hydroarylation. *ACS Catal.* **8**, 6079–6085 (2018).
- Yamano, R., Shibata, Y. & Tanaka, K. Synthesis of single and double dibenzohelicenes by rhodium-catalyzed intramolecular [2+2+2] and [2+1+2+1] cycloaddition. *Chem. Eur. J.* **24**, 6364–6370 (2018).
- González-Fernández, E. et al. Enantioselective synthesis of [6]carbohelicenes. *J. Am. Chem. Soc.* **139**, 1428–1431 (2017).
- Sanchez, I. G. et al. Oxahelicene NHC ligands in the asymmetric synthesis of nonracemic helicenes. *Chem. Commun.* **53**, 4370–4373 (2017).
- Jančařík, A. et al. Rapid access to dibenzohelicenes and their functionalized derivatives. *Angew. Chem. Int. Ed.* **52**, 9970 (2013).
- Metrano, A. J. & Miller, S. J. Peptide-based catalysts reach the outer sphere through remote desymmetrization and atroposelectivity. *Acc. Chem. Res.* **52**, 199–215 (2019).
- Wang, Y.-B. & Tan, B. Construction of axially chiral compounds via asymmetric organocatalysis. *Acc. Chem. Res.* **51**, 534–547 (2018).
- Zilate, B., Castrogiovanni, A. & Sparr, C. Catalyst-controlled stereoselective synthesis of atropisomers. *ACS Catal.* **8**, 2981–2988 (2018).
- Link, A. & Sparr, C. Stereoselective arene formation. *Chem. Soc. Rev.* **47**, 3804–3815 (2018).
- Loxq, P., Manoury, E., Poli, R., Deydier, E. & Labande, A. Synthesis of axially chiral biaryl compounds by asymmetric catalytic reactions with transition metals. *Coord. Chem. Rev.* **308**, 131–190 (2016).
- Liu, C.-X., Gu, Q. & You, S.-L. Asymmetric C–H bond functionalization of ferrocenes: new opportunities and challenges. *Trends Chem.* **2**, 737–749 (2020).
- Gao, D.-W., Gu, Q., Zheng, C. & You, S.-L. Synthesis of planar chiral ferrocenes via transition-metal-catalyzed direct C–H bond functionalization. *Acc. Chem. Res.* **50**, 351–365 (2017).
- Arae, S. & Ogasawara, M. Catalytic asymmetric synthesis of planar-chiral transition-metal complexes. *Tetrahedron Lett.* **56**, 1751–1761 (2015).
- Dhbaibi, K., Favereau, L. & Crassous, J. Enantioenriched Helicenes and Helicenoids Containing Main-Group Elements (B, Si, N, P). *Chem. Rev.* **119**, 8846–8953 (2019).
- Li, C., Yang, Y. & Miao, Q. Recent progress in chemistry of multiple helicenes. *Chem. Asian J.* **13**, 884–894 (2018).
- Lina, W.-B., Lia, M., Fanga, L. & Chen, C.-F. Recent progress on multidimensional construction of helicenes. *Chin. Chem. Lett.* **29**, 40–46 (2018).
- Shen, Y. & Chen, C.-F. Helicenes: synthesis and applications. *Chem. Rev.* **112**, 1463–1535 (2012).
- Wang, Y. et al. Gold-catalyzed asymmetric intramolecular cyclization of N-allenamides for the synthesis of chiral tetrahydrocarbolines. *Angew. Chem. Int. Ed.* **56**, 15905–15909 (2017).
- Chen, M. et al. Polymer-bound chiral gold-based complexes as efficient heterogeneous catalysts for enantioselectivity tunable cycloaddition. *ACS Catal.* **5**, 7488–7492 (2015).
- Zhang, Z.-M. et al. A new type of chiral sulfonamide monophosphate ligands: stereodivergent synthesis and application in enantioselective gold(I)-catalyzed cycloaddition reactions. *Angew. Chem. Int. Ed.* **53**, 4350–4354 (2014).
- Mato, M., Franchino, A., Garcia-Morales, C. & Echavarren, A. M. Gold-catalyzed synthesis of small rings. *Chem. Rev.* <https://doi.org/10.1021/acs.chemrev.0c00697> (2020). Recent reviews on asymmetric gold catalysis.
- Hendrich, C. M., Sekine, K., Koshikawa, T., Tanaka, K. & Hashmi, A. S. K. Homogeneous and Heterogeneous Gold Catalysis for Materials Science. *Chem. Rev.* <https://doi.org/10.1021/acs.chemrev.0c00824> (2020).
- Li, Y., Li, W. & Zhang, J. Gold-catalyzed enantioselective annulations. *Chem. Eur. J.* **23**, 467–512 (2017).
- Christian, A. H., Niemeyer, Z. L., Sigman, M. S. & Toste, F. D. Uncovering subtle ligand effects of phosphines using gold(I) catalysis. *ACS Catal.* **7**, 3973–3978 (2017).
- Zia, W. & Toste, F. D. Recent advances in enantioselective gold catalysis. *Chem. Soc. Rev.* **45**, 4567–4589 (2016).
- Dorel, R. & Echavarren, A. M. Gold(I)-catalyzed activation of alkynes for the construction of molecular complexity. *Chem. Rev.* **115**, 9028–9072 (2015).
- Qian, D. & Zhang, J. Gold-catalyzed cyclopropanation reactions using a carbenoid precursor toolbox. *Chem. Soc. Rev.* **44**, 677–698 (2015).
- Zhang, P.-C., Wang, Y., Qian, D., Li, W. & Zhang, J. Synthesis of **1** via the Sonogashira coupling reaction of *o*-ferrocenyl-bromo(iodo)benzene with 1-ethynyl-2-alkoxynaphthalene. *Chin. J. Chem.* **35**, 849 (2017).
- Mu, D. et al. Streamlined construction of silicon-stereogenic silanes by tandem enantioselective C–H silylation/alkene hydrosilylation. *J. Am. Chem. Soc.* **142**, 13459–13468 (2020).
- Hu, Y. et al. Organocatalytic asymmetric C(sp²)–H allylic alkylation: enantioselective synthesis of tetrasubstituted allenolates. *Angew. Chem. Int. Ed.* **59**, 19820–19824 (2020).
- Gu, X.-W. et al. Stereospecific Si–C coupling and remote control of axial chirality by enantioselective palladium-catalyzed hydrosilylation of maleimides. *Nat. Commun.* **11**, 2904 (2020).
- Liu, P. et al. Simultaneous control of central and helical chiralities: expedient helicoselective synthesis of dioxo[6]helicenes. *J. Am. Chem. Soc.* **142**, 16199–16204 (2020).
- Ma, C. et al. Atroposelective access to oxindole-based axially chiral styrenes via the strategy of catalytic kinetic resolution. *J. Am. Chem. Soc.* **142**, 15686–15696 (2020).

49. Romero-Arenas, A. et al. Ir-Catalyzed atroposelective desymmetrization of heterobiaryls: hydroarylation of vinyl ethers and bicycloalkenes. *J. Am. Chem. Soc.* **142**, 2628–2639 (2020).
50. Lu, S. et al. Diastereo- and atroposelective synthesis of bridged biaryls bearing an eight-membered lactone through an organocatalytic cascade. *J. Am. Chem. Soc.* **141**, 17062–17067 (2019).
51. Urbano, A., del Hoyo, A. M., Martínez-Carrión, A. & Carreño, M. C. Asymmetric synthesis and chiroptical properties of enantiopure helical ferrocenes. *Org. Lett.* **21**, 4623–4627 (2019).
52. Kamikawa, K. et al. Simultaneous induction of axial and planar chirality in arene-chromium complexes by molybdenum-catalyzed enantioselective ring-closing metathesis. *Chem. Eur. J.* **21**, 4954–4957 (2015). Only one example of axial and planar chiral arene chromium complexes via asymmetric catalysis.
53. Li, H., Jia, P., Qian, N., Li, S. & Jiao, P. Simultaneous construction of planar and central chiralities as well as unprecedented axial chirality on and around a ferrocene backbone. *J. Org. Chem.* **84**, 2817–2828 (2019). Axial and planar chiral ferrocene derivatives via multi-step synthesis using chiral substrate.
54. Wang, H. et al. Pd-catalyzed enantioselective syntheses of trisubstituted allenes via coupling of propargylic benzoates with organoboronic acids. *J. Am. Chem. Soc.* **142**, 9763–9771 (2020). For Ming-Phos ligands.
55. Xu, B. et al. Copper(I)/Ming-Phos-catalyzed asymmetric intermolecular [3+2] cycloaddition of azomethine Ylides with α -Trifluoromethyl α , β -unsaturated esters. *ACS Catal.* **7**, 210–214 (2017).
56. Zhang, Z.-M., Xu, B., Xu, S., Wu, H.-H. & Zhang, J. Diastereo- and enantioselective copper(I)-catalyzed intermolecular [3+2] cycloaddition of azomethine ylides with β -trifluoromethyl β , β -disubstituted enones. *Angew. Chem. Int. Ed.* **55**, 6324–6328 (2016).
57. Zhou, L. et al. Enantioselective difunctionalization of alkenes by a palladium-catalyzed heck/sonogashira sequence. *Angew. Chem. Int. Ed.* **59**, 2769–2775 (2020). For Xu-Phos ligands.
58. Zhu, C., Chu, H., Li, G., Ma, S. & Zhang, J. Pd-catalyzed enantioselective heck reaction of Aryl triflates and alkynes. *J. Am. Chem. Soc.* **141**, 19246–19251 (2019).
59. Zhang, Z.-M. et al. Enantioselective dicarbofunctionalization of unactivated alkenes by palladium-catalyzed tandem heck/suzuki coupling reaction. *Angew. Chem. Int. Ed.* **58**, 14653–14659 (2019).
60. Zhang, Z.-M. et al. Palladium/XuPhos-catalyzed enantioselective carboiodination of olefin-tethered aryl iodides. *J. Am. Chem. Soc.* **141**, 8110–8115 (2019).
61. Zhang, Z.-M. et al. Palladium-catalyzed enantioselective reductive heck reactions: convenient access to 3,3-disubstituted 2,3-dihydrobenzofuran. *Angew. Chem. Int. Ed.* **57**, 10373–10377 (2018).
62. Wang, L. et al. Enantioselective synthesis of isoxazolines enabled by palladium-catalyzed carboetherification of alkenyl oximes. *Angew. Chem. Int. Ed.* **59**, 4421–4427 (2020).
63. Tao, M. et al. Pd/Xiang-Phos-catalyzed enantioselective intermolecular carboheterofunctionalization under mild conditions. *Chem. Sci.* **11**, 6283–6288 (2020).
64. Zhang, P.-C., Wang, Y., Zhang, Z.-M. & Zhang, J. Gold(I)/Xiang-Phos-catalyzed asymmetric intramolecular cyclopropanation of indenones and trisubstituted alkenes. *Org. Lett.* **20**, 7049–7052 (2018).
65. Hu, H. et al. Enantioselective gold-catalyzed intermolecular [2+2]-cycloadditions of 3-styrylindoles with N-allenyl oxazolidinone. *Org. Chem. Front.* **3**, 759–763 (2016).
66. Chu, H., Cheng, J., Yang, J., Guo, Y.-L. & Zhang, J. Asymmetric dearomatization of indole by palladium/PC-Phos-catalyzed dynamic kinetic transformation. *Angew. Chem. Int. Ed.* **59**, 21991–21996 (2020).
67. Zhang, P.-C., Han, J. & Zhang, J. Pd/PC-Phos-catalyzed enantioselective intermolecular denitrogenative cyclization of benzotriazoles with allenes and N-allenamides. *Angew. Chem. Int. Ed.* **58**, 11444–11448 (2019).
68. Wang, L., Chen, M., Zhang, P., Li, W. & Zhang, J. Palladium/PC-Phos-catalyzed enantioselective arylation of general sulfenate anions: scope and synthetic applications. *J. Am. Chem. Soc.* **140**, 3467–3473 (2018).
69. Lin, T.-Y. et al. Design and synthesis of TY-Phos and application in palladium-catalyzed enantioselective fluoroarylation of gem-difluoroalkenes. *Angew. Chem. Int. Ed.* **59**, 22957–22962 (2020).
70. Jia, M. & Bandini, M. Counterion effects in homogeneous gold catalysis. *ACS Catal.* **5**, 1638–1652 (2015). Coordinating ability of different counterions associated with active gold catalysts can also significantly modulate their electrophilic nature.
71. Chen, Y., Yekta, S. & Yudin, A. K. Modified BINOL ligands in asymmetric catalysis. *Chem. Rev.* **103**, 3155–3212 (2003). The potential applications of the axial and planar chiral naphthol **3** is interest in asymmetric catalysis and material sciences, see,
72. Li, Y., Manickam, G., Ghoshal, A. & Subramaniam, P. More efficient palladium catalyst for hydrogenolysis of benzyl groups. *Synth. Commun.* **36**, 925–928 (2006).
73. Zhao, Y. & Truhlar, D. G. The M06 suite of density functionals for main group thermochemistry, thermochemical kinetics, noncovalent interactions, excited states, and transition elements: two new functionals and systematic testing of four M06-class functionals and 12 other functionals. *Theor. Chem. Acc.* **120**, 215–241 (2008).
74. Frisch, M. J. et al. *Gaussian 09*, Revision D.01; (Gaussian, Inc., 2009).
75. Dunning Jr, T. H. & Hay, P. J. In *Modern Theoretical Chemistry*, H. F. Schaefer III 3rd edn, 1–28 (Plenum, 1977).
76. Fuentealba, P., Preuss, H., Stoll, H. & Szentpály, L. V. A proper account of core-polarization with pseudopotentials: single valence-electron alkali compounds. *Chem. Phys. Lett.* **89**, 418–422 (1982).
77. Marenich, A. V., Cramer, C. J. & Truhlar, D. G. Universal solvation model based on solute electron density and on a continuum model of the solvent defined by the bulk dielectric constant and atomic surface tensions. *J. Phys. Chem. B* **113**, 6378–6396 (2009).
78. Truhlar, D. G. & Gordon, M. S. From force fields to dynamics: classical and quantal paths. *Science* **249**, 491–498 (1990).
79. Gonzalez, C. & Schlegel, H. B. An improved algorithm for reaction path following. *J. Chem. Phys.* **90**, 2154–2161 (1989).

Acknowledgements

We gratefully acknowledge the funding support of NSFC (22031004, 21921003), Shanghai Municipal Education Commission (20212308), and the postdoctoral research fund CPSF (2019M661420). We greatly appreciate Ph.D. Yanfei Niu at East China Normal University for her kind help with X-ray single crystal structural analyses, M.S. Lian-Fang Yang at East China Normal University for her kind help with NMR structural analyses.

Author contributions

J.Z., P.-C.Z., and H.-H.W., conceived the project, analyzed the data and wrote the paper. P.-C.Z., performed the most of experiments. Y.-L.L. and J.H. helped in synthesis of substrates **1**. Z.L. did the DFT calculations. All authors discussed the results and commented on the paper.

Competing interests

The authors declare no competing interests.

Additional information

Supplementary information The online version contains supplementary material available at <https://doi.org/10.1038/s41467-021-24678-5>.

Correspondence and requests for materials should be addressed to H.-H.W., Z.L. or J.Z.

Peer review information *Nature Communications* thanks Peng Jiao and the other anonymous reviewer(s) for their contribution to the peer review of this work. Peer reviewer reports are available.

Reprints and permission information is available at <http://www.nature.com/reprints>

Publisher's note Springer Nature remains neutral with regard to jurisdictional claims in published maps and institutional affiliations.



Open Access This article is licensed under a Creative Commons

Attribution 4.0 International License, which permits use, sharing, adaptation, distribution and reproduction in any medium or format, as long as you give appropriate credit to the original author(s) and the source, provide a link to the Creative Commons license, and indicate if changes were made. The images or other third party material in this article are included in the article's Creative Commons license, unless indicated otherwise in a credit line to the material. If material is not included in the article's Creative Commons license and your intended use is not permitted by statutory regulation or exceeds the permitted use, you will need to obtain permission directly from the copyright holder. To view a copy of this license, visit <http://creativecommons.org/licenses/by/4.0/>.

© The Author(s) 2021